







Studies on Physical, Mechanical and Tribological Properties of Al6063 Incorporated with CNT & Nano Clay as Filler Materials

Asifiqbal M. Doddamani^{a,*} , Iresh G. Bhavi^b , R. Noorahmed^c , Mohan B. Vanarotti^d ,
J. Balaji^e , Syed Sameer Hussain^a 

^aDepartment of Mechanical Engineering, SECAB Institute of Engineering and Technology, VTU, Belgaum, Karnataka, India,
^bDepartment of Mechanical Engineering, BLDEA's V. P. Dr. P. G. Halakatti College of Engineering and Technology, VTU, Belgaum, Karnataka, India,
^cDepartment of Mechanical Engineering, M.S College of Engineering, VTU, Belgaum Karnataka, India,
^dDepartment of Mechanical Engineering, Kolhapur Institute of Technology's, College of Engineering, Kolhapur, Maharashtra, India,
^eDepartment of Mechanical Engineering, Dr Ambedkar Institute of Technology, VTU, Belgaum, Karnataka, India.

Keywords:

Al6063 alloy
Carbon nano tube (CNT)
Nano clay (NC)
Mechanical properties
Tribological properties
Hybrid reinforced composite

* Corresponding author:

Asifiqbal M. Doddamani
E-mail: asif.d12@gmail.com

Received: 9 September 2024
Revised: 6 October 2024
Accepted: 18 November 2024



ABSTRACT

In order to improve mechanical and tribological qualities, this study investigates the innovative use of stir-casting to integrate carbon nanotubes (CNT) and nano clay (NC) as dual reinforcement materials in Al6063 matrix composites. Combining CNT (0–2%) with NC (0–2%) in a synergistic way presents a special chance to capitalise on each filler material's particular properties. With an increase in CNT and NC on the Al6063 matrix, mechanical parameters like tensile strength, hardness, flexural strength, and compressive strength rise from 225-245 MPa, 45-74 BHN, 218-298 MPa, and 140-152 MPa. Tribological characteristics were analyzed through pin on disc (tribometer), with varying loads (5 N - 10 N), velocity (0.209 m/s - 1.047 m/s) and sliding distance (253.32-753.98 m). The results demonstrate that the addition of 2 wt% CNT and 2 wt% NC reduces the specific wear rate value and increase the coefficient of friction. A decrease of wear rate value 0.0162 mm³/m and increase in COF 0.70 was observed at maximum load of 10 N and velocity of 0.209 m/s corresponding to 2 wt% of CNT and NC incorporation. The homogeneous distribution of fillers in the metal matrix, tensile fracture, distinct wear modes, and the importance of CNT/NC in changing the wear process from abrasion to delamination are all demonstrated by SEM analysis.

© 2024 Published by Faculty of Engineering

1. INTRODUCTION

Metal matrix composite (MMC) have attracted significant interest in material science and

engineering because they offer the possibility of merging the lightweight attributes of metals with the exceptional mechanical and tribological properties of reinforcing materials [1]. Al6063, a

versatile aluminum alloy, combined with a hybrid reinforcement of CNTs and Nanoclay, is relatively unique. This combination leverages the high mechanical strength and load transfer capabilities of CNTs, along with the lubricating properties and high surface area of Nanoclay makes the composite surface smooth, which together improve the specific wear rate and mechanical properties.

Powder metallurgy, liquid metal stir casting, and squeeze casting are three processes that have been investigated for integrating ceramic particles into aluminium matrices. Each of these processes has advantages and disadvantages, but we chose stir casting because of its ability to evenly disperse nano ceramic particles within the aluminium alloy matrix. Stir casting, unlike other processes, is a cost-effective and scalable approach that maintains composite structural uniformity. This contrast from previous efforts emphasises our method's significance and the justification for its use in this investigation. Powder metallurgy is more expensive due to the cost of producing metal powders and the need for specialized equipment. Although PM provides better precision, it is generally not as scalable for high-volume production compared to stir casting. Stir casting is often favored for its simplicity and cost-effectiveness in producing large components, while powder metallurgy offers superior material properties and precision but at a higher cost and for more specialized applications.

Aluminum-based alloys, including Al-6063, have been thoroughly studied among the many MMCs for use in sectors that demand increased strength and wear resistance. This study investigates a novel method of using carbon nanotubes (CNT) and nano clay (NC) as hybrid filler materials to progress the exhibition of Al6063 [2-3]. Carbon nanotubes are renowned for their exceptional mechanical strength, enabling efficient load transfer from the matrix to the fillers, while Nanoclay offers a high surface area and lubricating properties, resulting in a smoother composite surface and reduced specific wear rate (SWR) [4]. By integrating these two distinct filler materials, a comprehensive enhancement strategy is envisaged, addressing the multifaceted challenges encountered in both mechanical and tribological aspects [5]. Several studies have underscored the promising outcomes of incorporating CNTs in metal matrices, demonstrating drastically progress

in tensile, hardness, and impact resistance [6-7]. Likewise, the utilization of nano clay as a reinforcing agent has exhibited notable advancements in wear resistance and tribological performance [8]. However, the synergistic effects arising from the simultaneous integration of CNT and nano clay in Al-6063 matrix composites remain largely unexplored [9-10]. Explores the impact of varying powder metallurgy parameters on the tribological performance and micro-hardness of Al6063 aluminum matrix composites (MMCs) reinforced with nano Al_2O_3 particles. Through controlled adjustments to processing conditions, the study examines how these parameters influence wear resistance, hardness, and overall composite performance. This research provides valuable insights for optimizing material properties in aluminum-based MMCs for enhanced durability and mechanical functionality [11]. Formed an Al 7075/Al2O3 composite via the liquid metallurgy process and introduced Gr particles to examine their impact on wear properties. Findings revealed that Gr-reinforced composites exhibited superior wear strength compared to Al 7075/Al2O3 composites [12-16]. The outcome demonstrates that Al7075 alloy composites reinforced with SiC and Gr content have a lower wear rate. According to the study, graphite creates a lubricating coating while SiC acts as a load-bearing component, creating a smoother composite surface and a higher coefficient of friction [17]. When the investigator compares the wear resistance of pristine Al2024 alloy to reinforced Sic and Gr with Al2024 composite alloy, he notices a significant increase in wear resistance of the hybrid composite alloy [18]. The metal matrix AA6026 is mixed with the hybrid fillers carbon fiber and nano-clay at varying weight percentages between 1 and 5%. The outcome demonstrates that adding 3% of nanoclay improves the mechanical attributes of the composite [19]. The researcher discovered that the CNT-reinforced matrix AA6061 had a steady friction coefficient, a 22% enhances in tensile strength, and a 3% deficit in elongation [20]. The stir casting method is a more comfortable and simple way to make aluminium metal matrix composites when it comes to fabrication [21-25]. Magnesium was added to the aluminium metal matrix composite formed by the forging, extrusion, and heat treatment processes to improve its wet ability. As a result, the coefficient of friction increased and the wear rate decreased [26]. The reinforcing material and mould cabin are

preheated to the necessary temperature in order to minimize oxidation, in order to enhance the reinforcement' interactions with Metal matrix alloy to improve mechanical and wear characteristics [27]. Because of their increased wear resistance, reinforced aluminium matrix compositions are thought to be the ideal low density material in the electronics, automotive, marine, and aerospace industries [28-30]. Aluminium matrix composition is used in the automotive sector for moving parts of engines, transmissions, brake systems, and vehicle structural assemblies [31-33].

The most potential use of aluminium (MMC) over time is the replacement of conventional auto materials in braking system and lightweight components such as auto engines, such as steel, and cast iron [34-37]. This work examined the use of hydrogel nano composites as adsorbents for the removal of RY dye. These nano composites were created utilizing AAC and NIPAM polymers along with MMT nano fillers [52]. The flame fragmentation deposition method, which uses homemade equipment to synthesize under appropriate pressure conditions, is the most effective way for producing MWCNT [53]. This evaluation is on using the flame fragments deposition (FFD) approach to create synthetic carbon nanotubes (CNTs). This technology is simple, inexpensive, and allows for the preparation of CNTs at lower temperatures than other conventional methods [54]. The brilliant green (BG) dye is absorbed by the ZnO/CNT nano composite, a more effective adsorbent than commercially available adsorbent, in the treatment of waste water [55].

This research builds upon the existing knowledge by systematically investigating the cooperative influence of CNT and nano clay on the Tribological and mechanical attributes of Al-6063. Experimental approach includes a detailed examination of tensile strength, hardness, impact resistance, friction, and wears resistance under various conditions. The findings of this investigation not only add to the fundamental perceptive of MMCs but also present a pathway for designing high-performance materials tailored for applications demanding robust mechanical and tribological characteristics. Similarly, nano clay has garnered attention for its high surface area and lubricating capabilities, making it a valuable candidate for enhancing

wear resistance in composite materials. However, the simultaneous integration of CNT and nano clay in Al-6063 composites remains an underexplored territory. The proposed research seeks to address this gap by systematically investigating the cooperative effects of these hybrid fillers on both mechanical and tribological properties. The work builds upon the foundations laid by previous studies, aiming to provide a comprehensive understanding of the micro-structural evolution induced by the synergistic combination of CNT and nano clay in the Al-6063 matrix by using SEM.

2. MATERIALS & METHODS

2.1 Material

The current investigation addresses the tribological and mechanical attributes of Al-6063 incorporated with carbon nanotubes (CNT) and nano clay (NC) as filler materials, the average size is 50 nm as shown in figure 1 and experimental methodology follows a systematic process. The Al-6063 powder is first carefully weighed as the base material, alongside the chosen CNT and NC fillers. The CNT and NC were purchased from Ultra nanotech private limited, Bengaluru, India The Al6063 was purchased from Belmont industrial solutions, Bengaluru, India.

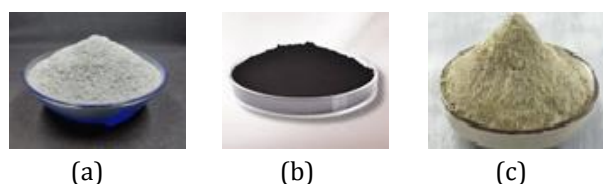


Fig. 1. (a) Al6063, (b) Carbon nanotubes, (c) Nano clay.

2.2 Method

In this study, we employ the stir casting technique as shown in figure 2 it offers a straightforward and cost-effective approach for the fabrication of Aluminum hybrid reinforced matrix-composites. The process begins by dividing approximately 800 grams of the base metal into chips, subsequently undergoing a 60-minute heating period in the furnace until it reaches 720°C. Simultaneously, the reinforcement particles Carbon nano tube and Nano clay are placed in separate crucibles and preheated in a furnace for 30 minutes, achieving a temperature of 250°C. Once the base metal attains

a molten state, the preheated reinforcement particles are introduced, and the amalgamation process commences. Stirring is done at 250-rpm speed for approximately 10 (minutes), ensuring a thorough and homogeneous mixture. This methodology is chosen not only for its simplicity but also for its efficiency in producing high-quality Aluminium hybrid metal matrix composites. To evaluate the efficacy of the CNT and nanoclay reinforcements, the finished composite material is characterized for attributes such as tensile strength, hardness, compression, flexural, wear resistance, and micro-structural characterization. Table 1 and Table show the physical and chemical properties of Al6063 metal alloy. Table 3 depicts the specimen chemical-composition of Al6063 hybrid reinforced matrix composites.

Table 1. Physical properties of Al6063.

Material	Density gm/cc ³	Melting point	Modulus of elasticity GPa	Poisson's ratio
Al6063	2.7	655°	68.9	0.33



Fig. 2. Stir casting Furnace with electric heater.

Table 2. Al6063 Chemical-Composition in wt % [38].

Element	Composition (%)
Si	0.2 -- 0.6
Fe	0.35
Cu	0.1
Mn	0.1
Mg	0.45 -- 0.9
Zn	0.1
Ti	0.1
Cr	0.1
Al	Balance

Table 3. Specimen Composition.

Specimen No.	Composition (%)
S1	Al6063
S2	Al6063+0.5% NC+0.5%CNT
S3	Al6063+1.0% NC+1.0%CNT
S4	Al6063+1.5% NC+1.5%CNT
S5	Al6063+2.0% NC+2.0%CNT

2.3 Physical, Mechanical and Tribological characterization of reinforced composites Density and void fraction

The rule-of-mixture (see Eq. (1)) is used to compute the theoretical density of CNT and NC combined with Al-6063 metal alloy composites. The Archimedes principle is then used to evaluate the experimental density. Following that, void content is determined using equation (2).

$$\rho_{th} = \frac{1}{\frac{W_m}{\rho_m} + \frac{W_{r1}}{\rho_{r1}} + \frac{W_{r2}}{\rho_{r2}}} \quad (1)$$

Void-fraction=

$$\left(\frac{\text{Theoretical density}(\rho_{th}) - \text{Experimental density}(\rho_{exp})}{\text{Theoretical density}(\rho_{th})} \right) \quad (2)$$

Tensile strength

A basic mechanical test called a tensile test Stir-casting were used to produce the tensile test samples in accordance with ASTM E8/E8M. The comprehensive methods for performing room-temperature tensile testing on metallic materials are provided by this standard. Tensile testing determines a material's yield strength, ultimate tensile strength, elongation, and area reduction by measuring the material's resistance to breaking under tension. The specimen, which has dimensions of 115 mm in total length, 10 mm in the head diameter with 30 mm in length, and 6 mm in the inner diameter with 55 mm in length, resembles a dog bone. With the load cell, a load of roughly 0.1 mm/mm/minute was applied.

Hardness

Using a Brinell hardness testing machine, the hardness value of the manufactured particle mixed Al6063 metal alloy composites is ascertained. For measures of hardness, a polished specimen of the composite measuring 10 X 10 X 25 mm³ was collected. The hardness of a specimen is measured using a metal ball indenter. A minor load of 10 kgf is applied to the specimen, and a major load of 100 kgf is applied

to the hardness examination specimen to determine the BHN value. The Brinell hardness testing machine's read dial provides an accurate indication of the examined specimen's hardness.

Flexural strength

The Flexural test gauges how manufactured composite materials behave when subjected to basic flexural loads. For the flexural test, an ASTM E-290 standard specimen measuring 60 mm in length and 10 mm by 10 mm in cross-section is ready. The Universal Testing Machine (UTM) with a 40 mm span length is used to conduct the flexural test. The specimen is positioned as simply supported at the middle of the span, and focused stress is applied using the three-point beam bending technique. The UTM dial indication provides a direct reading of the focused load, which steadily rises until the beam is intact.

Compressive strength

The ASTM E9-09-prepared sample for the compression test has a dimension of 10X10X30 mm³. The specimen is fixed between the UTM's two jaws. When a compressive stress is given to a specimen by a moveable jaw, the specimen's length reduces and its cross-sectional area rises. This process is known as swelling. The UTM dial indication is used to read the reading immediately after the specimen fails the compression test.

Wear Test

Wear investigation is conducted on pin-on-disc (Figure 3a) wear and Friction monitor apparatus which employs essentially the basic 'tribometer', test rigs. The end of the specimen (Figure 3c) diameter 10 mm and length 32 mm as per G-99, rides on the disc surface of 165mm diameter and 8 mm thickness. The volume of wear of the pin specimen is computed from the weight-loss measured and the density. Throughout the experiment, the specimen slides against a rotating disc with a 50 mm track radius. The standard load of 5, 7.5, and 10 N is delivered to the rotating disc in a downward direction. During the wear test, the force transducer is used to determine the friction force. The steel disc that is rotating is below the force transducer. Using an electronic (Figure 3d) balance, the mass of each sample is tabulated both before & after the test. The least count on the electric balance is 0.0001gm. With the specimen fixed on the pin holder, the machine runs on

changing settings including weight, sliding distance, and speed (Figure 3b). The sample's mass loss is computed as the difference between the experiment's starting and end weights. By dividing the mass loss by the density, the volume loss is further transformed. The sample's volume loss aids in determining how the reinforcement addition to the matrix alloy affects the composite's resistance to wear.



(a)



(b)



(c)



(d)

Fig. 3. (a) Pin on disc apparatus, (b) Top view of Specimen holding on disc, (c) Specimens, (d) Specimen weighing balance.

The specific wear rate is calculated by using equation 3.

$$W_s = \frac{\Delta m}{\rho \times V_s \times t \times F_n} \tag{3}$$

Whereas W_s —wear rate $\text{mm}^3/\text{N}\cdot\text{m}$, Δm = mass lost during trial in gm, ρ = density of composition in g/cm^3 , V_s = rotating disk speed m/s , t = duration of test, F_n = load (N).

Co-efficient of friction

The coefficient of friction is a dimensionless number that measures the resistance to motion when two surfaces make contact. It is the ratio of the frictional force between two objects to the normal force that holds them together. This coefficient changes according to the nature of the surfaces in contact and is classified into two types: static and dynamic friction. Static friction is the barrier to the start of motion, whereas kinetic friction occurs when surfaces are already moving against one other. A larger coefficient indicates more resistance to movement, whereas a lower value provides smoother interactions. The coefficient of friction is a key idea in comprehending and forecasting motion in mechanical systems since it can be influenced by variables including material composition, surface roughness, and the presence of lubricants

Micro structure analysis

Scanning electron microscopy was used to provide a comprehensive examination of the microstructure of reinforced Al6063 alloy composites. Uniformly distribution of two fillers with Al6063 matrix alloy. Details on heat treatment, reinforced material composition in mechanical terms, wear rate and phase distribution, content incorporation, and structural flaws are provided by surface morphology, examining engineering component cracks, fractures, and other flaws.

3 RESULTS & DISCUSSION

3.1 Density & void fraction

From specimen S1 to specimen S5, the Table 4 data show a pattern of increasing porosity or voids. Both the growing percentages of void fraction (0.74 to 2.10 %) and the expanding gap between theoretical and experimental densities show this. As the weight percentage of CNT and

NC particles increases, so does the void content. The existence of an air bubble and porosity during the alloy's filler material mixing process is the cause of the variations in the void content of the composites. The mechanical and wear properties suffer greatly when voids are present. This may be the result of a number of things, including inconsistent manufacturing practices, deteriorating materials, or additional processing variables that require more research to guarantee material quality.

Table 4 Void fraction of CNT and NC with Al6063 alloy composites.

Specimen No.	Theoretical density (g/cc ³)	Experimental density (g/cc ³)	Void-fraction (%)
S1	2.70	2.68	0.74
S2	2.693	2.667	0.97
S3	2.686	2.656	1.12
S4	2.679	2.639	1.49
S5	2.672	2.616	2.10

3.2 Tensile strength

The tensile strength of Al-6063 with CNT and NC was measured using UTM in accordance with ASTM standards. The specimen is moulded to the required dog bone shape and measurement. The varied specimens are tested using ASTM standards, and the results are shown in Figure 4 that the tensile strength increases from 225 MPa to 243 MPa, indicating that the fillers engage and form intermolecular bonds with Al6063.

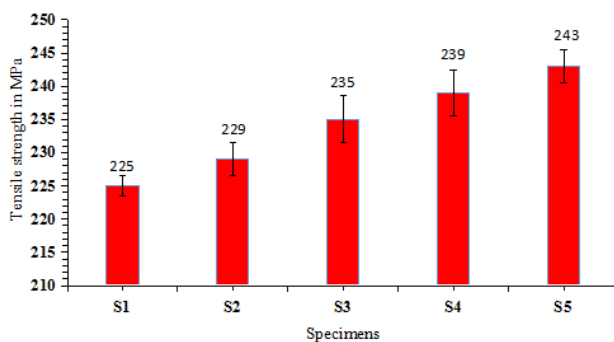


Fig. 4. Tensile strength of reinforced Al6063 composite.

The Al6063 alloy specimen (S1) has a tensile strength of 225 MPa, but the hybrid filler specimen (S2) has a tensile strength of 229 MPa because the fillers restrict the movement of the Al6063 molecular atoms. Similarly the S2 to S5 reinforced composites show the tensile strength was drastically going up by almost 9 % due to

the uniform distribution of fillers CNT/Nanoclay, and these materials are act as the load bearer and avoid the dislocation moment of Al6063 alloy matrix [49]. This reinforced material reduces ductility and enhances brittleness phase and porosity.

3.3 Hardness

The hardness test is performed to determine the material's indentation resistance. Figure 5 indicates that the hardness increases from 45 BHN for neat Al6063 to 74 BHN for hybrid reinforced Al6063 alloy composite.

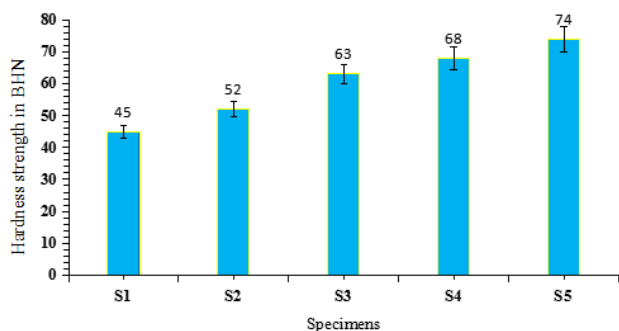


Fig. 5. Hardness of reinforced Al6063 composite.

The hardness increase due to the combination of CNT and NC have good intermolecular connection with the metal matrix, CNT improves hardness as well as tough material, which resists the indentation load and improves the hardness from 52 to 74 BHN. The specimen S2 has a BHN value 52 BHN greater than the neat Al6063, indicating that the filler material CNT and NC content raises the BHN value of the specimen (S2). This two filler acts as a binder for Al6063 metal alloy composite and they can withstand the indentation.

3.4 Flexural strength

Figure 6 shows the figures for the hybrid reinforced Al6063 alloy matrix's flexural strength. The Al6063 alloy (S1), when compared to the reinforced composite samples S2 and S3, has the highest strength (140 MPa) because of the uneven distribution of CNT/Nanoclay within the Al6063 matrix. Flexural strength increased as the amount of CNT/Nanoclay nano fillers increased in samples S4 and S5, as shown in Fig. 3C. This is because CNT/Nanoclay avoids the moment of dislocation and improves the elastic modulus of the Al6063 alloy matrix composites, which leads to a significant improvement in flexural strength [50].

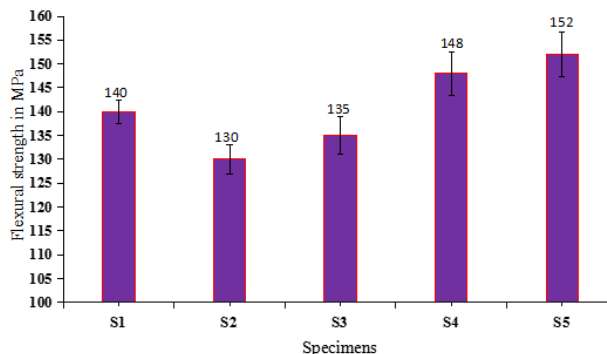


Fig. 6. Flexural strength of reinforced Al6063 composite.

3.5 Compressive

Figure 7 shows a plot of the compressive strength values for the Al6063 alloy and its reinforced composite. Compared to the other samples, S2 through S5, the Al6063 alloy sample S1 has the lowest compressive value of 218 MPa. As the amount of CNT/Nanoclay nano hard ceramic content rose in the Al6063 alloy matrix, the hardness property of the filler prevented the alloy matrix's dislocation moment, which continued to enhance compressive strength. It was noted in prior research, investigator found that the compressive strength of reinforced composite increases to 298 MPa [51].

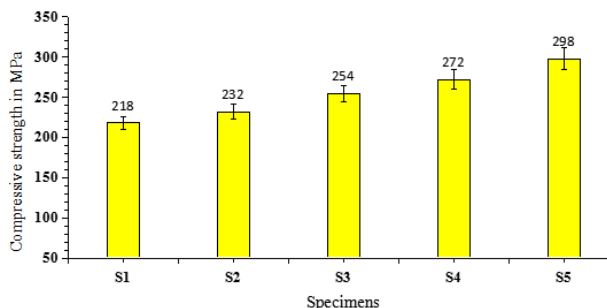


Fig. 7. Compressive strength of reinforced Al6063 composite.

3.6 Wear rate

The Fig 8 shows the relationship between wear rate (in mm³/m) v/s load (in N), Velocity (m/s) and sliding distance (m) for five distinct samples (S1, S2, S3, S4, and S5). It was analyzed that the wear rate of reinforced composites (S2 to S5) was lower than the Al6063 alloy matrix (S1). Fig. 8a shows how applied normal load affects the wear rates in reinforced composites and the Al6063 alloy. It is clear that both the Al6063 alloy and the reinforced composites experience an increase in wear rate as the applied load increases.

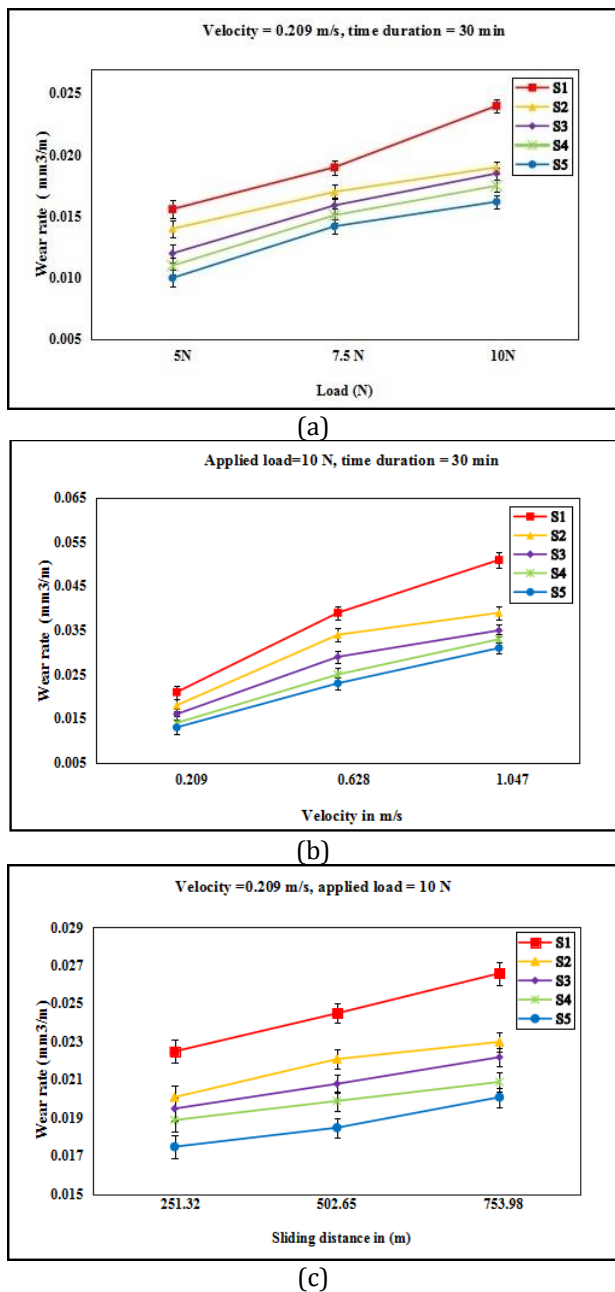


Fig. 8. (a) Wear-rate v/s load, (b) Wear-rate v/s Velocity, c) Wear-rate v/s sliding-distance.

On the other hand, under all measured loads, the reinforced composites show consistently lower wear rates than the Al6063 alloy. The higher degree of plastic deformation in both the Al6063 alloy and in reinforced composites explains the rise in wear rate with increasing load. Greater plastic deformation raises the possibility of subsurface cracking, which outcome in a larger loss of material. Greater plastic deformation raises the possibility of subsurface cracking, which results in a larger loss of material [39]. Delamination can also lead to enhanced amounts of wear in the Al6063 alloy and the reinforced

composites. Delamination can be caused by an increased load. The consequence of sliding velocity on the wear rate of in reinforced composites and Al 6063 alloy is shown in Figure 8b. It is clear that for both the Al6063 alloy and the in reinforced alloy composites, the wear rate increases with increasing sliding velocity. According to [40], this rise can be ascribed to the increased strain rate that is producing subsurface deformation. Increased contact areas and delamination are caused by the fracture and fragmentation of asperities brought on by the enhanced subsurface deformation rate, which increases wear loss. All evaluated sliding velocities, however, show that the in reinforced composites show consistently lower rate of wear than the Al6063 alloy. The consequence of sliding velocity on the wear rate of in reinforced composites and Al 6063 alloy is shown in Figure 8b. It is clear that for both the Al6063 alloy and the in reinforced alloy composites, the wear rate increases with increasing sliding velocity. According to [40], this rise can be ascribed to the increased strain rate that is producing subsurface deformation. Increased contact areas and delamination are caused by the fracture and fragmentation of asperities brought on by the enhanced subsurface deformation rate, which increases wear loss. All evaluated sliding velocities, however, show that the in reinforced composites show consistently lower rate of wear than the Al6063 alloy.

Figure 8c shows that the rate of wear in reinforced composites and the Al6063 alloy gradually increases with the sliding distance, eventually reaching a steady state above 502.65 meters. The more intimate contact that develops over time between the specimen's sliding surfaces and the revolving disc is what causes the wear rate to increase with sliding distance. Wear is further exacerbated by the material being pushed into a plastic condition by the temperature rising at the specimen-disc contact as the sliding distance increases. Other studies have observed similar observations [41,42].

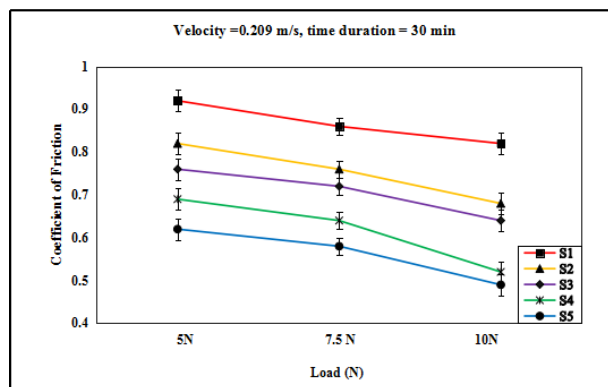
3.7 Coefficient of friction (COF)

The Figure 9 depicts coefficient of friction of in reinforced composites is found to significantly decrease as the amount of CNT and nanoclay increases. When compared to the Al6063 alloy, the composite sample (S2 to S5) of CNT and

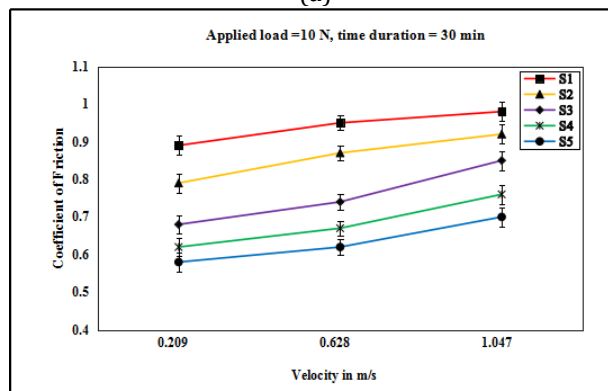
nanoclay, respectively, show a decrease in coefficient of friction. Researchers [43] have documented a similar tendency. The fact that uniformly dispersed CNT and nanoclay particles operate as load bearers throughout the sliding process may possibly contribute to the reinforced composites' improved ant frictional performance. Since the reinforced particles are said to function as load-bearing components [44,45], friction between the disc surface and CNT/Nanoclay should have been the primary source of friction.

The influence of normal load on the coefficient of friction for the in reinforced composites and the Al6063 alloy is shown in Figure 9a. The coefficient of friction of the generated in reinforced composites and the Al6063 alloy both exhibit a discernible decrease with increasing load. For all loads examined, the reinforced composites continuously show lower coefficients of friction than the Al6063 alloy. Furthermore, the COF gradually decreases for both the Al6063 alloy and the reinforced combination up to a load of 10 N, after which there is no discernible change. One explanation for this behaviour is the existence of subsequent phases. Components such as CNT and nanoclay in composites act to restrict metal movement during sliding [43]. The coefficient of friction may be further decreased at greater loads when softened debris bits take on the role of solid lubricants [46]. For composites, higher load causes more CNT/Nanoclay to be transferred to the mating and sliding surfaces, improving lubrication at the sliding interface. Furthermore, because of the tight link between the reinforcement and matrix that result can withstand larger loads with minimum plastic deformation.

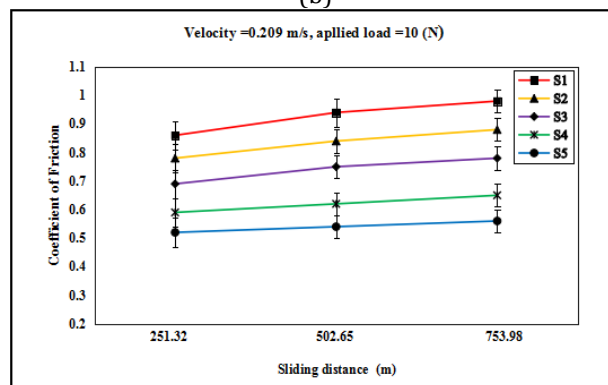
Fig. 9b shows how sliding velocity affects Al6063 alloy's coefficient of friction as well as reinforced composites'. The thin adherent solid lubricating coating results from broken brittle particle reinforcements in the composites being pushed out onto matrix a surface that lowers the coefficient of friction. This is why it is observed that the coefficient of friction increases with increasing sliding velocity for both the Al6063 alloy and the reinforced composites. The occurrence of this phenomenon accelerates with higher sliding velocities. The temperature of the mating surfaces [47] also causes more asperity junctions at higher velocities, which raises the coefficient of friction.



(a)



(b)



(c)

Fig. 9. (a) Co-efficient of friction v/s load, (b) Co-efficient of friction v/s Velocity, (c) Co-efficient of friction v/s sliding distance.

Figure 9c illustrates the relationship between sliding-distance and COF for Al6063 alloy reinforced composites. It is found that the coefficient of friction increases slightly and consistently with increasing sliding distance for both the reinforced composites and the A6063 alloy. CNT act as the load barrier and transfer the load from matrix to the fillers and nanoclay forms lubricating film on the composites which helps in smooth surface so that the friction is very less, which generates low frictional-force. Other academics have also noted similar findings [48]. However, an at all

tested sliding distance, the reinforced composites' coefficient of friction reduces as the concentration of CNT/Nanoclay increases.

3.8 Microstructure analysis

SEM study was critical for determining the alloy's micro-structural features, which can affect its mechanical and tribological qualities of Al6063 with CNT, and NC as shown in Fig 10 respectively. Using SEM equipment, the microstructure of fracture of the flexural and tensile surfaces of specimens (S1 and S4) was examined (Fig. 10a-d).

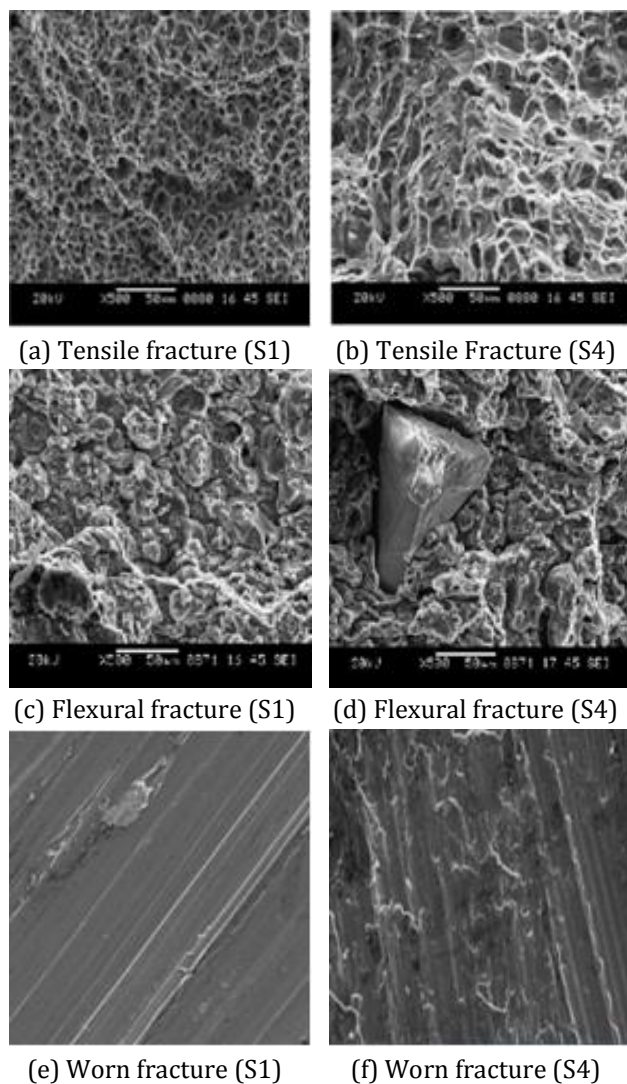


Fig.10. Micro structural Analysis and Interaction Study of Pure Al6063 (S1) and Specimen (S4).

In pristine Al6063, abrasive and adhesive wear as well as torn particles were clearly visible (Fig. 10a&c). Particle reinforced S4 specimens did not exhibit these adhesive and

abrasive wear patterns or ripped particles buried to the matrix surface (Fig 10b&d). Furthermore, ductile fracture was found at these stir casting samples because of their non-porous structure when the microstructure of tensile and flexural fracture surface specimens was examined using a scanning electron microscope. The SEM analysis showed fine collaborating bond between the Al6063 matrix and the reinforcements. This strong bonding is crucial for load always relocate from the matrix to the reinforcements, thereby enhancing the composite's mechanical properties. Aluminum-based particle-reinforced metal matrix composites have a thin, porous, spongy, and non-bright structure, plastic deformation, groove creation on their surfaces, and noticeably better wear resistance.

The worn tracks seen on the surface of the pristine Al6063 alloy and the reinforced Al6063/1.5 percent CNT/1.5% NC composite are displayed in Figs. 10(e & f). The immaculate Al6063 S1's wear track is examined in detail in Fig. 10e, where it is noted that abrasive wear has caused furrows and some scratches to appear on the matrix alloy's worn surface at 10 N. The wear track of the reinforced Al6063 composite is displayed in Fig. 10f, revealing characteristics mostly related to the abrasive mechanism. Since there aren't many indications of worn debris adhered to the specimen S4's surface, it is clear that adhesive wear is less severe than abrasive wear.

4. CONCLUSIONS

The current research project uses the stir-casting technique to produce aluminium alloy composite samples that contain CNT/Nanoclay nano ceramic particles.

- It is analyzed from the experimentation that the density of Al6063 alloy decreases by adding 2 wt % of CNT & 2 wt % of Nanoclay when compare to pristine alloy due to low density of nanoclay.
- The Al6063/2%CNT/2%NC composite (specimen 5) has got an increase in hardness of 74 BHN value as compared to the pristine Al6063 alloy of 45 BHN.

- There are improvement in the tensile, compression and flexural strength for the Al6063/2%CNT/2%NC (specimen 5) composite 243 MPa, 298 MPa and 152 MPa as compared to pristine alloy value 225 MPa, 218MPa and 140 MPa respectively. It is due to hybrid filler which restricts the movement of molecules of Al6063 alloy.
- At all loads under consideration, the specific wear rate (SWR) is found to be minimum for the Al603/25CNT/2%NC composite (specimen 5) is 0.0162 mm³/m under the condition of load 10KN, velocity of 0.209 m/s and duration of 30 mints. The maximum coefficient of friction of composite (specimen 5) value 0.70 under the condition of velocity is 0.209 m/s. load=10 KN and sliding distance =753.98 m. CNT act as load barrier and nanoclay act as a lubricating film on the composite, so that the wear rate decreases and friction increases at particular condition.

On overall perspective it can be concluded that the specimen 5 ha got the highest tensile, hardness, compression, flexural strength and coefficient of friction but specific wear rate is minimum.

Acknowledgement

The Department of Mechanical Engineering, SECAB Institute of Engineering and Technology, Vijayapura, Karnataka, are to be thanked for granting a sponsorship for the purchase, fabrication, and testing of specimens. For their assistance in carrying out the research, I also acknowledge R&D, the Department of Mechanical Engineering, SECAB Institute of Engineering and Technology, Vijayapura.

REFERENCES

- [1] Z. Li et al., "Enhanced Mechanical Properties of Graphene (Reduced GrapheneOxide)/Aluminum Composites with a Bioinspired Nanolaminated Structure," *Nano Letters*, vol. 15, no. 12, pp. 8077–8083, Nov. 2015, doi: [10.1021/acs.nanolett.5b03492](https://doi.org/10.1021/acs.nanolett.5b03492).
- [2] B. Guo et al., "Exploiting the synergic strengthening effects of stacking faults in carbon nanotubes reinforced aluminum matrix composites for enhanced mechanical properties," *Composites Part B Engineering*, vol. 211, p. 108646, Jan. 2021, doi: [10.1016/j.compositesb.2021.108646](https://doi.org/10.1016/j.compositesb.2021.108646).
- [3] S. Liu, V. S. Chevali, Z. Xu, D. Hui, and H. Wang, "A review of extending performance of epoxy resins using carbon nanomaterials," *Composites Part B Engineering*, vol. 136, pp. 197–214, Sep. 2017, doi: [10.1016/j.compositesb.2017.08.020](https://doi.org/10.1016/j.compositesb.2017.08.020).
- [4] M. Maurya, S. Kumar, and V. Bajpai, "Assessment of the mechanical properties of aluminium metal matrix composite: A review," *Journal of Reinforced Plastics and Composites*, vol. 38, no. 6, pp. 267–298, Dec. 2018, doi: [10.1177/0731684418816379](https://doi.org/10.1177/0731684418816379).
- [5] T. S. Srivatsan, W. C. Harrigan Jr, and S. H. Murph, *Metal-Matrix Composites: Advances in Analysis, Measurement, and Observations*. Springer Nature, 2021.
- [6] D. K. Koli, G. Agnihotri, and R. Purohit, "A review on properties, behaviour and processing methods for Al- Nano Al₂O₃ composites," *Procedia Materials Science*, vol. 6, pp. 567–589, Jan. 2014, doi: [10.1016/j.mspro.2014.07.072](https://doi.org/10.1016/j.mspro.2014.07.072).
- [7] B. Zhu, T. Bai, P. Wang, Y. Wang, C. Liu, and C. Shen, "Selective dispersion of carbon nanotubes and nanoclay in biodegradable poly(ϵ -caprolactone)/poly(lactic acid) blends with improved toughness, strength and thermal stability," *International Journal of Biological Macromolecules*, vol. 153, pp. 1272–1280, Nov. 2019, doi: [10.1016/j.ijbiomac.2019.10.262](https://doi.org/10.1016/j.ijbiomac.2019.10.262).
- [8] P. Azhagiri, N. Senthilkumar, K. Palanikumar, and B. Deepanraj, "Mechanical properties evaluation on hybrid AA6026 composites added with nanoclay and carbon fibers," *Carbon Letters*, vol. 33, no. 3, pp. 833–846, Jan. 2023, doi: [10.1007/s42823-023-00464-9](https://doi.org/10.1007/s42823-023-00464-9).
- [9] D. S. Prakash, V. Balaji, D. Rajesh, P. Anand, and M. Karthick, "Experimental investigation of nano reinforced aluminium based metal matrix composites," *Materials Today Proceedings*, vol. 54, pp. 852–857, Nov. 2021, doi: [10.1016/j.matpr.2021.11.189](https://doi.org/10.1016/j.matpr.2021.11.189).
- [10] K. J. Lijay, J. D. R. Selvam, I. Dinaharan, and S. J. Vijay, "Microstructure and mechanical properties characterization of AA6061/TiC aluminum matrix composites synthesized by in situ reaction of silicon carbide and potassium fluotitanate," *Transactions of Nonferrous Metals Society of China*, vol. 26, no. 7, pp. 1791–1800, Jul. 2016, doi: [10.1016/s1003-6326\(16\)64255-3](https://doi.org/10.1016/s1003-6326(16)64255-3).
- [11] S. Haque, M. A. Rahman, R. R. Shaikh, N. Sirajudeen, M. B. Kamaludeen, and O. Sahu, "Effect of powder metallurgy process parameters on tribology and micro hardness of Al6063- nano Al₂O₃ MMCs," *Materials Today Proceedings*, vol. 68, pp. 1030–1037, Jan. 2022, doi: [10.1016/j.matpr.2022.08.255](https://doi.org/10.1016/j.matpr.2022.08.255).

- [12] I. Sabry and A. M. Hewidy, "Underwater friction-stir welding of a stir-cast AA6061-SiC metal matrix composite: optimization of the process parameters, microstructural characterization, and mechanical properties," *Materials Science-Poland*, vol. 40, no. 1, pp. 101–115, Mar. 2022, doi: [10.2478/msp-2022-0013](https://doi.org/10.2478/msp-2022-0013).
- [13] A. Baradeswaran and A. E. Perumal, "Study on mechanical and wear properties of Al 7075/Al₂O₃/graphite hybrid composites," *Composites Part B Engineering*, vol. 56, pp. 464–471, Aug. 2013, doi: [10.1016/j.compositesb.2013.08.013](https://doi.org/10.1016/j.compositesb.2013.08.013).
- [14] J. Balaji, M. M. Nataraja, K. Sadashiva, and S. Supreeth, "Experimental and Computational Analysis of Thermal Characteristics of Polymer Resin Reinforced with Rice Husk and Aluminium Nitride Filler Composites," *Journal of the Institution of Engineers (India) Series D*, vol. 105, no. 1, pp. 313–321, Apr. 2023, doi: [10.1007/s40033-023-00480-z](https://doi.org/10.1007/s40033-023-00480-z).
- [15] E. S. Esakkiraj, S. Suresh, N. S. V. Moorthi, M. K. Kumar, and S. M. J. Ranjith, "Study of Mechanical Behaviour of Stir Cast Aluminium Based Composite Reinforced with Mechanically Ball Milled TiB₂ Nano Particles," *Advanced Materials Research*, vol. 984–985, pp. 410–415, Jul. 2014, doi: [10.4028/www.scientific.net/amr.984-985.410](https://doi.org/10.4028/www.scientific.net/amr.984-985.410).
- [16] S. Suresh, N. S. V. Moorthi, S. C. Vettivel, and N. Selvakumar, "Mechanical behavior and wear prediction of stir cast Al–TiB₂ composites using response surface methodology," *Materials & Design (1980-2015)*, vol. 59, pp. 383–396, Mar. 2014, doi: [10.1016/j.matdes.2014.02.053](https://doi.org/10.1016/j.matdes.2014.02.053).
- [17] R. Kumar and S. Dhiman, "A study of sliding wear behaviors of Al-7075 alloy and Al-7075 hybrid composite by response surface methodology analysis," *Materials & Design (1980-2015)*, vol. 50, pp. 351–359, Mar. 2013, doi: [10.1016/j.matdes.2013.02.038](https://doi.org/10.1016/j.matdes.2013.02.038).
- [18] S. Suresha and B. K. Sridhara, "Effect of silicon carbide particulates on wear resistance of graphitic aluminium matrix composites," *Materials & Design (1980-2015)*, vol. 31, no. 9, pp. 4470–4477, May 2010, doi: [10.1016/j.matdes.2010.04.053](https://doi.org/10.1016/j.matdes.2010.04.053).
- [19] P. Azhagiri, N. Senthilkumar, K. Palanikumar, and B. Deepanraj, "Mechanical properties evaluation on hybrid AA6026 composites added with nanoclay and carbon fibers," *Carbon Letters*, vol. 33, no. 3, pp. 833–846, Jan. 2023, doi: [10.1007/s42823-023-00464-9](https://doi.org/10.1007/s42823-023-00464-9).
- [20] A. Sharma, H. Fujii, and J. Paul, "Influence of reinforcement incorporation approach on mechanical and tribological properties of AA6061- CNT nanocomposite fabricated via FSP," *Journal of Manufacturing Processes*, vol. 59, pp. 604–620, Oct. 2020, doi: [10.1016/j.jmapro.2020.10.016](https://doi.org/10.1016/j.jmapro.2020.10.016).
- [21] P. Morampudi, V. S. N. V. Ramana, C. Prasad, K. SriramVikas, and N. Rahul, "Physical, mechanical and corrosion properties of Al6061/ZrB₂ metal matrix nano composites via powder metallurgy process," *Materials Today Proceedings*, vol. 59, pp. 1708–1713, Jan. 2022, doi: [10.1016/j.matpr.2022.03.596](https://doi.org/10.1016/j.matpr.2022.03.596).
- [22] A. A. Emiru, D. K. Sinha, A. Kumar, and A. Yadav, "Fabrication and Characterization of Hybrid Aluminium (Al6061) Metal Matrix Composite Reinforced with SiC, B₄C and MoS₂ via Stir Casting," *International Journal of Metalcasting*, vol. 17, no. 2, pp. 801–812, May 2022, doi: [10.1007/s40962-022-00800-1](https://doi.org/10.1007/s40962-022-00800-1).
- [23] M. S. Surya, "Effect of SiC weight percentage and sintering duration on microstructural and mechanical behaviour of AL6061/SiC composites produced by Powder Metallurgy Technique," *Silicon*, vol. 14, no. 6, pp. 2731–2739, Mar. 2021, doi: [10.1007/s12633-021-01053-z](https://doi.org/10.1007/s12633-021-01053-z).
- [24] S. Dhanesh, K. S. Kumar, N. K. M. Fayiz, L. Yohannan, and R. Sujith, "Recent developments in hybrid aluminium metal matrix composites: A review," *Materials Today Proceedings*, vol. 45, pp. 1376–1381, Jul. 2020, doi: [10.1016/j.matpr.2020.06.325](https://doi.org/10.1016/j.matpr.2020.06.325).
- [25] S. Sivananthan, V. R. Reddy, and C. S. J. Samuel, "Preparation and evaluation of mechanical properties of 6061Al-Al₂O₃ metal matrix composites by stir casting process," *Materials Today Proceedings*, vol. 21, pp. 713–716, Aug. 2019, doi: [10.1016/j.matpr.2019.06.744](https://doi.org/10.1016/j.matpr.2019.06.744).
- [26] S. A. Hasan, M. U. Zaki, and F. Hasan, "Properties & characterization of reinforced aluminium metal matrix composites," *Materials Today Proceedings*, Feb. 2023, doi: [10.1016/j.matpr.2023.01.307](https://doi.org/10.1016/j.matpr.2023.01.307).
- [27] B. C. Kandpal, J. Kumar, and H. Singh, "Fabrication and characterisation of Al₂O₃/aluminium alloy 6061 composites fabricated by Stir casting," *Materials Today Proceedings*, vol. 4, no. 2, pp. 2783–2792, Jan. 2017, doi: [10.1016/j.matpr.2017.02.157](https://doi.org/10.1016/j.matpr.2017.02.157).
- [28] M. P. Chakravarthy and D. S. Rao, "Evaluation of mechanical properties of aluminium alloy (AA 6082) reinforced with Rice husk ash (RHA) and Boron carbide (B₄C) hybrid metal matrix composites using stir casting method," *Materials Today Proceedings*, vol. 66, pp. 580–586, Jan. 2022, doi: [10.1016/j.matpr.2022.06.293](https://doi.org/10.1016/j.matpr.2022.06.293).

- [29] S. T. Mavhungu, E. T. Akinlabi, M. A. Onitiri, and F. M. Varachia, "Aluminum Matrix Composites for industrial use: Advances and trends," *Procedia Manufacturing*, vol. 7, pp. 178–182, Dec. 2016, doi: [10.1016/j.promfg.2016.12.045](https://doi.org/10.1016/j.promfg.2016.12.045).
- [30] V. Srinivasan, S. Kunjiappan, and P. Palanisamy, "A brief review of carbon nanotube reinforced metal matrix composites for aerospace and defense applications," *International Nano Letters.*, vol. 11, no. 4, pp. 321–345, Mar. 2021, doi: [10.1007/s40089-021-00328-y](https://doi.org/10.1007/s40089-021-00328-y).
- [31] V. Chak, H. Chattopadhyay, and T. L. Dora, "A review on fabrication methods, reinforcements and mechanical properties of aluminum matrix composites," *Journal of Manufacturing Processes*, vol. 56, pp. 1059–1074, Jun. 2020, doi: [10.1016/j.jmapro.2020.05.042](https://doi.org/10.1016/j.jmapro.2020.05.042).
- [32] C. Elanchezhian, B. V. Ramanth, G. B. Bhaskar, and M. Vivekanandhan, "An investigation of the mechanical properties of HybridComposites in applications of automotive industry," *Materials Today Proceedings*, vol. 16, pp. 875–882, Jan. 2019, doi: [10.1016/j.matpr.2019.05.172](https://doi.org/10.1016/j.matpr.2019.05.172).
- [33] P. D. Srivyas and Charoo, "Application of hybrid aluminum matrix composite in automotive industry," *Materials Today Proceedings*, vol. 18, pp. 3189–3200, Jan. 2019, doi: [10.1016/j.matpr.2019.07.195](https://doi.org/10.1016/j.matpr.2019.07.195).
- [34] M. P. Chakravarthy and D. S. Rao, "Evaluation of mechanical properties of aluminium alloy (AA 6082) reinforced with Rice husk ash (RHA) and Boron carbide (B4C) hybrid metal matrix composites using stir casting method," *Materials Today Proceedings*, vol. 66, pp. 580–586, Jan. 2022, doi: [10.1016/j.matpr.2022.06.293](https://doi.org/10.1016/j.matpr.2022.06.293).
- [35] S. T. Mavhungu, E. T. Akinlabi, M. A. Onitiri, and F. M. Varachia, "Aluminum Matrix Composites for industrial use: Advances and trends," *Procedia Manufacturing*, vol. 7, pp. 178–182, Dec. 2016, doi: [10.1016/j.promfg.2016.12.045](https://doi.org/10.1016/j.promfg.2016.12.045).
- [36] V. Srinivasan, S. Kunjiappan, and P. Palanisamy, "A brief review of carbon nanotube reinforced metal matrix composites for aerospace and defense applications," *International Nano Letters.*, vol. 11, no. 4, pp. 321–345, Mar. 2021, doi: [10.1007/s40089-021-00328-y](https://doi.org/10.1007/s40089-021-00328-y).
- [37] V. Chak, H. Chattopadhyay, and T. L. Dora, "A review on fabrication methods, reinforcements and mechanical properties of aluminum matrix composites," *Journal of Manufacturing Processes*, vol. 56, pp. 1059–1074, Jun. 2020, doi: [10.1016/j.jmapro.2020.05.042](https://doi.org/10.1016/j.jmapro.2020.05.042).
- [38] P. Paramasivam and S. Vijayakumar, "Mechanical characterization of aluminium alloy 6063 using destructive and non-destructive testing," *Materials Today Proceedings*, vol. 81, pp. 965–968, May 2021, doi: [10.1016/j.matpr.2021.04.312](https://doi.org/10.1016/j.matpr.2021.04.312).
- [39] F. Akhtar, "Microstructure evolution and wear properties of in situ synthesized TiB₂ and TiC reinforced steel matrix composites," *Journal of Alloys and Compounds*, vol. 459, no. 1–2, pp. 491–497, May 2007, doi: [10.1016/j.jallcom.2007.05.018](https://doi.org/10.1016/j.jallcom.2007.05.018).
- [40] A. A. Hamid, P. K. Ghosh, S. C. Jain, and S. Ray, "The influence of porosity and particles content on dry sliding wear of cast in situ Al(Ti)–Al₂O₃(TiO₂) composite," *Wear*, vol. 265, no. 1–2, pp. 14–26, Dec. 2007, doi: [10.1016/j.wear.2007.08.018](https://doi.org/10.1016/j.wear.2007.08.018).
- [41] I. M. Hutchings, "Tribological properties of metal matrix composites," *Materials Science and Technology*, vol. 10, no. 6, pp. 513–517, Jun. 1994, doi: [10.1179/mst.1994.10.6.513](https://doi.org/10.1179/mst.1994.10.6.513).
- [42] T. Ma, H. Yamaura, D. A. Koss, and R. C. Voigt, "Dry sliding wear behavior of cast SiC-reinforced Al MMCs," *Materials Science and Engineering A*, vol. 360, no. 1–2, pp. 116–125, Jul. 2003, doi: [10.1016/s0921-5093\(03\)00408-8](https://doi.org/10.1016/s0921-5093(03)00408-8).
- [43] S. Kumar, M. Chakraborty, V. S. Sarma, and B. S. Murty, "Tensile and wear behaviour of in situ Al–7Si/TiB₂ particulate composites," *Wear*, vol. 265, no. 1–2, pp. 134–142, Dec. 2007, doi: [10.1016/j.wear.2007.09.007](https://doi.org/10.1016/j.wear.2007.09.007).
- [44] M. Godet, "The third-body approach: A mechanical view of wear," *Wear*, vol. 100, no. 1–3, pp. 437–452, Dec. 1984, doi: [10.1016/0043-1648\(84\)90025-5](https://doi.org/10.1016/0043-1648(84)90025-5).
- [45] S. Basavarajappa, G. Chandramohan, A. Mahadevan, M. Thangavelu, R. Subramanian, and P. Gopalakrishnan, "Influence of sliding speed on the dry sliding wear behaviour and the subsurface deformation on hybrid metal matrix composite," *Wear*, vol. 262, no. 7–8, pp. 1007–1012, Nov. 2006, doi: [10.1016/j.wear.2006.10.016](https://doi.org/10.1016/j.wear.2006.10.016).
- [46] M. Kestursatya, J. K. Kim, and P. K. Rohatgi, "Friction and wear behavior of a centrifugally cast lead-free copper alloy containing graphite particles," *Metallurgical and Materials Transactions A*, vol. 32, no. 8, pp. 2115–2125, Aug. 2001, doi: [10.1007/s11661-001-0023-z](https://doi.org/10.1007/s11661-001-0023-z).
- [47] F. Rana and D. M. Stefanescu, "Friction properties of Al-1.5 Pct Mg/SiC particulate metal-matrix composites," *Metallurgical Transactions A*, vol. 20, no. 8, pp. 1564–1566, Aug. 1989, doi: [10.1007/bf02665513](https://doi.org/10.1007/bf02665513).

- [48] H. Goto and S. Takaki, "Friction and Wear Characteristics of Al-Si Alloy Impregnated Graphite Composite under Lubricated Sliding Conditions," *The Proceedings of Conference of Kyushu Branch*, vol. 2003.56, pp. 225–226, Jan. 2003, doi: [10.1299/jsmekyushu.2003.56.225](https://doi.org/10.1299/jsmekyushu.2003.56.225).
- [49] G. G. Sirata, K. Waclawiak, and A. J. Dolata, "Microstructure and Mechanical Properties of the EN AC-ALSi12CuNiMg Alloy and AlSi Composite Reinforced with SiC Particles," *Archives of Foundry Engineering*, Feb. 2024, doi: [10.24425/afe.2024.149271](https://doi.org/10.24425/afe.2024.149271).
- [50] T. Arunkumar, V. Pavanan, V. A. Murugesan, V. Mohanavel, and K. Ramachandran, "Influence of nanoparticles reinforcements on aluminium 6061 alloys fabricated via novel ultrasonic aided Rheo-Squeeze casting method," *Metals and Materials International*, vol. 28, no. 1, pp. 145–154, May 2021, doi: [10.1007/s12540-021-01036-0](https://doi.org/10.1007/s12540-021-01036-0).
- [51] V. Gholipour, M. Shamanian, A. Ashrafi, and A. Maleki, "Development of Aluminium-Nanoclay composite by using powder metallurgy and hot extrusion process," *Metals and Materials International*, vol. 27, no. 9, pp. 3681–3694, Jul. 2020, doi: [10.1007/s12540-020-00791-w](https://doi.org/10.1007/s12540-020-00791-w).
- [52] N. D. Radia, M. A. Muninir, S. M. Essa, and A. M. Aljeboree, (2024). "Removal of Reactive Yellow Dye from Aqueous Solutions Using Hydrogel Nano-composites Based on Montmorillonite Clay," *Advanced Journal of Chemistry, Section A*, vol. 7, no. 6, pp. 725-739. Nov. 2024. doi: [10.48309/ajca.2024.462420.1547](https://doi.org/10.48309/ajca.2024.462420.1547).
- [53] A. M. Jassm, F. H. Hussein, F. H. Abdulrazzak, A. F. Alkaim, and B. A. Joda, "Synthesis and characterization of carbon nanotubes by modified flame fragments deposition Method," *Asian Journal of Chemistry*, vol. 29, no. 12, pp. 2804–2808, Jan. 2017, doi: [10.14233/ajchem.2017.20994](https://doi.org/10.14233/ajchem.2017.20994).
- [54] S. S. Mahmood, A. A. Atiya, F. H. Abdulrazzak, A. F. Alkaim and F. H. Hussein, "Review on Applications of Carbon Nanotubes (CNTs) in Solar Cells," *Journal of Medicinal and Chemical Sciences*, vol 4, no. 3, pp. 225-229, May 2021. doi: [10.26655/jmchemsci.2021.3.2](https://doi.org/10.26655/jmchemsci.2021.3.2)
- [55] A. M. Aljeboree, S. A. Hussein, M. A. Jawad, and A. F. Alkaim, "Hydrothermal synthesis of eco-friendly ZnO/CNT nanocomposite and efficient removal of Brilliant Green cationic dye," *Results in Chemistry*, vol. 7, p. 101364, Jan. 2024, doi: [10.1016/j.rechem.2024.101364](https://doi.org/10.1016/j.rechem.2024.101364).